Mon. Not. R. Astron. Soc. **000**, 1–4 (2012) Printed 24 September 2012 (MN LATEX style file v2.2)

What can we gain from magnification bias as a complement to shear?

Christopher Duncan[1], Alan Heavens[2], Catherine Heymans[1], Benjamin Joachimi[1]
[1] *Institute for Astronomy, Royal Observatory Edinburgh, Blackford Hill, Edinburgh*
[2] *Imperial College London*

Submitted

ABSTRACT
With the wealth of upcoming data from wide-field surveys such as KiDS, Pan-STARRS, DES and Euclid, it is more important than ever to understand the full range of independent probes of cosmology at our disposal. With this in mind, we motivate the use of cosmic magnification as a probe of cosmology, presenting forecasts for the improvements to cosmic shear cosmological parameter constraints when cosmic magnification is included for a KiDS-like survey. We find that when uncertainty in the galaxy bias is factored into the forecasts, cosmic magnification is less powerful that previously reported, but as it is less likely to be prone to measurement error we conclude it is a useful tool for cosmological analyses.

Key words: gravitational lensing: weak, magnification, shear – cosmology

1 INTRODUCTION

As light from distant galaxies propagates through the Universe, its path can be deflected by the local matter distribution, an effect called gravitational lensing. As a result, when we view images of distant galaxies we observe both a change in the shape of the image as well as a change in its size. The former of these effects is described by shear, and statistical analyses of cosmic shear have proven to be a very promising tool in constraining cosmology. However, as cosmic shear analysis requires accurate shape information of observed galaxies, its measurement has proven a particularly difficult task **?**, with measurements sensitive to the Point Spread Function (PSF) and pixelisation, as well as physical contamination from intrinsic galaxy alignments.

The change in size of a body due to gravitational lensing is referred to as magnification. Whilst direct measurements of a change in sizes of a lensed galaxy population have been successful **?**, these can suffer from similar measurement systematics to cosmic shear and are less frequently used for statistical analyses using magnification. Instead, magnification can also be studied via its effect on the observed number density of sources, known as magnification bias. Detections using number density effects have been performed using the cross-correlation between low redshift galaxies and high redshift quasars **??**, and more recently with high redshift Lyman break galaxies **??**. Whilst weak magnification analyses via number density effects do not suffer from many of the systematics inherent in a shear analysis, they are affected however by their own set of systematics which have been less thoroughly studied.

2 TWO-POINT CORRELATIONS FROM MAGNIFICATION BIAS

2.1 Number Density Statistics

Deflection of light by intervening matter causes the observed number density of source bodies to be changed in two ways:

(i) The solid angle behind the lens is stretched by a factor of μ (where μ is the local magnification factor), thus the observed position of sources is changed leading to a dilution of sources behind a foreground over-density
(ii) The observed size of the source is changed, leading to an increase in the observed flux of the source as an application of Louiville's Theorem. The observed number density of sources may then change in a flux limited survey, as sources are (de-)amplified across this flux limit. This is equivalent to an effective change in the flux limit of the survey $S \rightarrow S/\mu$.

These two effects then modify the observed number counts of sources as

$$n(>S,\theta) = \frac{n_0(>S/\mu(\theta),\theta)}{\mu(\theta)}. \quad (1)$$

Assuming that the unlensed number counts follow a power law $n_0(>S) \propto S^{\alpha}$, equation (1) becomes:

$$n(>S) = \mu^{\alpha-1} n_0(>S) = (1+2(\alpha-1)\kappa(\theta))n_0(>S) \quad (2)$$

where the weak lensing approximation $\mu \sim 1+2\kappa$ has been used. From equation (2) it is clear that when $\alpha = 1$ the overall magnification effect does not cause a change in the observed number density of sources, as the dilution of sources is perfectly balanced by the amplification of sources. Alterna-

tively, when $\alpha \neq 1$ there will be an overall increase/reduction in the observed number of sources. It can be shown that

$$\alpha(m) = 2.5\frac{d\,log\,n(>m)}{dm} \quad (3)$$

where we have changed to magnitudes instead of fluxes. Defining the number density contrast as $\delta n = (n - n_0)/n_0$, equation (2) states the fluctuation in observed number density due to magnification follows

$$\delta n_M(\theta) = 2(\alpha - 1)\kappa(\theta) \quad (4)$$

and the observed number density contrast is then

$$\delta n^{(i)}(\theta) = \delta n_M^{(i)}(\theta) + \delta n_I^{(i)}(\theta) + \delta n_{rn}^{(i)}(\theta) \quad (5)$$

with δn_M the change in number density due to magnification, as given in equation (4), δn_I the contribution from the intrinsic clustering of the sources according to their dark matter environment, and δn_{rn} a random stochastic element. As surveys measure projected quantities across the sky, we consider projected number density contrast, defined for each term later, with redshift information from a tomographic analysis using photometric redshifts. Superscript in parenthesis denote a tomographic photo-z bin i.

As the convergence (and consequently number over-density) vanish when averaged over large scales, the observed number density satisfies $\langle n \rangle = \langle n_0 \rangle$, and we consider two point correlations of these quantities. In particular, we consider the two point correlation of the Fourier coefficients of the convergence and number density contrast, related to the Power Spectrum P as:

$$\langle x^{(i)}(\ell) x^{(j)}(\ell') \rangle = (2\pi)^2 \delta_D(\ell - \ell') P_{xx}^{(ij)}(\ell) \quad (6)$$

for variable x. $\delta_D(\ell - \ell')$ is the two dimensional Dirac delta function, which illustrates the non-mixing of angular wavenumber (ℓ) modes due to isotropy and homogeneity. Thus, from equation (5) we see that the observables in which we are interested follow:

$$P_{\delta n \delta n}^{(ij)}(\ell) = P_{MM}^{(ij)}(\ell) + P_{II}^{(ij)}(\ell) + P_{MI}^{(ij)}(\ell) + P_{IM}^{(ij)}(\ell) + \delta_K^{ij} S_{\delta n}^{(ij)} \quad (7)$$

$$P_{\kappa_s \kappa_s}^{(ij)}(\ell) = P_{\kappa\kappa}^{(ij)}(\ell) + \delta_K^{ij} S_{\kappa_s}^{(ij)} \quad (8)$$

$$P_{\kappa_s \delta n}^{(ij)}(\ell) = P_{\kappa I}^{(ij)}(\ell) + P_{\kappa M}^{(ij)}(\ell) \quad (9)$$

where δ_K^{ij} is the Kronecker delta function. For notational convenience I have suppressed the subscripts such that $\delta n_I \to I$ and $\delta n_M \to M$, and used the fact the stochastic term for the number density contrast and shear are uncorrelated with the other quantities and only contribute to the shot noise (S) in the autocorrelation term. When considering the shear-only signal, we assume that all the shape information is contained in the convergence field κ_s, defined as in equation (10). This should be a valid approximation as the shear and convergence power spectra are identical, $P_{\kappa\kappa} = P_{\gamma\gamma}$.

The projected convergence field is defined as

$$\kappa(\theta) = \int_0^{\chi_H} d\chi\, q^{(i)}(\chi) \delta_m(\theta, \chi) \quad (10)$$

with χ the comoving distance of the source, δ_m the dark matter over density, and the weight given as

$$q^{(i)}(\chi) = \frac{3H_0^2\Omega_m}{2c^2}\frac{f_K(\chi)}{a(\chi)}\int_\chi^{\chi_H} d\chi'\, p^{(i)}(\chi')\frac{f_K(\chi' - \chi)}{f_k(\chi')}. \quad (11)$$

$p^{(i)}(\chi)$ denotes the galaxy comoving distance probability distribution for tomographic redshift bin i, a the scale factor and $f_K(\chi)$ the angular diameter distance.

Similarly, the projected number density contrast due to intrinsic clustering is given by

$$\delta n_I(\theta) = \int_0^{\chi_H} d\chi'\, p^{(i)}(\chi) \delta n_I(\theta, \chi) \quad (12)$$

where the galaxy comoving distance probability distribution $p^{(i)}(\chi)$ is the same as that defined in (11). In using the same galaxy distribution in modelling the number density contrast as the shape convergence κ_s, we assume that the sample of galaxies used is restricted to those in which shape information is available, or that the galaxy distribution of the sample of galaxies used in shape measurement is representative of the galaxy distribution of the sample which may be used for magnification analysis. As shape measurement on a galaxy requires a higher signal to noise than required for magnification, we expect that a magnification analysis could use a larger sample of galaxies for surveys which take photometry on galaxies even when shape information cannot be resolved. This may be taken partly into account in the Shot Noise contribution to the number density contrast power spectrum, as described in Section ***, however we assume this has a negligible effect on the galaxy distribution.

The fluctuation due to intrinsic clustering is related to the matter over density via a bias term that can be scale or distance dependant, $\delta n_I(\theta, \chi) = b(\theta, \chi)\delta_m(\theta, \chi)$ so that the intrinsic clustering contribution to the power spectrum follows

$$P_{II}(k, z) = b^2(k, z) P_{\delta_m \delta_m}(k, z) \quad (13)$$

$$P_{I\delta_m}(k, z) = b(k, z) r(k, z) P_{\delta_m \delta_m}(k, z) \quad (14)$$

with $r(k, z)$ a stochastic bias which we take to be unity for the remainder of this paper.

All power spectra terms for projected quantities are related to the three dimensional dark matter power spectra using the Limber approximation in the flat sky limit. The contributions to the number density contrast power spectra in equation (7) are then

$$P_{\kappa\kappa}^{(ij)}(\ell) = \int_0^{\chi_H} d\chi\, \frac{q^{(i)}(\chi) q^{(j)}(\chi)}{f_K^2(\chi)} P_{\delta_m \delta_m}^{(ij)}\left(\frac{\ell}{f_K(\chi)}, \chi\right) = P_{\gamma\gamma}^{(ij)}(\ell) \quad (15)$$

$$P_{MM}^{(ij)}(\ell) = 4(\alpha^{(i)} - 1)(\alpha^{(j)} - 1) P_{\kappa\kappa}^{(ij)}(\ell) \quad (16)$$

$$P_{\kappa M}^{(ij)}(\ell) = 2(\alpha^{(j)} - 1) P_{\kappa\kappa}^{(ij)} \quad (17)$$

$$P_{MI}^{(ij)}(\ell) = 4(\alpha^{(i)} - 1)\int_0^{\chi_H} d\chi\, \frac{q^{(i)}(\chi) p^{(j)}(\chi)}{f_K^2(\chi)} \times b\left(\frac{\ell}{f_K(\chi)}, \chi\right) P_{\delta_m \delta_m}^{(ij)}\left(\frac{\ell}{f_K(\chi)}, \chi\right) \quad (18)$$

$$P_{IM}^{(ij)}(\ell) = 4(\alpha^{(j)} - 1)\int_0^{\chi_H} d\chi\, \frac{p^{(i)}(\chi) q^{(j)}(\chi)}{f_K^2(\chi)} \times b\left(\frac{\ell}{f_K(\chi)}, \chi\right) P_{\delta_m \delta_m}^{(ij)}\left(\frac{\ell}{f_K(\chi)}, \chi\right) \quad (19)$$

$$P_{II}^{(ij)}(\ell) = \int_0^{\chi_H} d\chi\, \frac{p^{(i)}(\chi) p^{(j)}(\chi)}{f_K^2(\chi)} \times b^2\left(\frac{\ell}{f_K(\chi)}, \chi\right) P_{\delta_m \delta_m}^{(ij)}\left(\frac{\ell}{f_K(\chi)}, \chi\right) \quad (20)$$

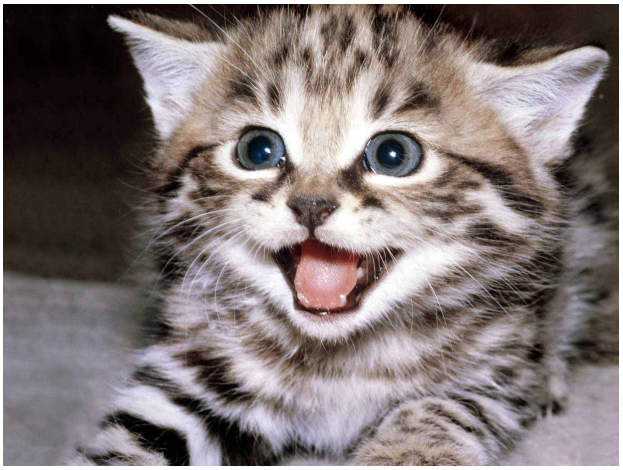

Figure 1. Contributions to the number density contrast power spectrum for a combination of redshift bins. Autocorrelation term contains Shot Noise. If possible, includes the shear PS and equivalent Shot Noise term

$$P_{\kappa I}^{(ij)}(\ell) = \int_0^{\chi_H} d\chi \, \frac{q^{(i)}(\chi)p^{(j)}(\chi)}{f_K^2(\chi)} \times b\left(\frac{\ell}{f_K(\chi)}, \chi\right) P_{\delta_m\delta_m}^{(ij)}\left(\frac{\ell}{f_K(\chi)}, \chi\right). \quad (21)$$

2.2 Shot Noise

The final contribution to the observed number density contrast power spectrum comes from the Shot Noise term, P_{SN} in equation (7), which is non-zero only when considering the autocorrelation, when $i = j$, and takes the form

$$S_{\delta n}^{(ij)} = \delta_K^{ij} \frac{1}{\bar{n}^{(i)}}. \quad (22)$$

When considering the shear-only signal, this is modified to

$$S_{\kappa_s}^{(ij)} = \delta_K^{ij} \frac{\sigma_\epsilon^2}{2\bar{n}^{(i)}} \quad (23)$$

where σ_ϵ is the intrinsic ellipticity dispersion per component, typically $\sigma_\epsilon \sim 0.4$.

2.3 Parameter Forecasts

To estimate parameter constraints we use a Fisher Matrix analysis, where the Fisher Matrix is given by

$$F_{\alpha\beta} = \sum_r \frac{\ell_r d\ell_r \Delta\Omega}{4\pi} Tr[C^{-1}(\ell_r)C_{,\alpha}(\ell_r)C^{-1}(\ell_r)C_{,\beta}(\ell_r)] \quad (24)$$

where $C(\ell)$ is the covariance matrix for data vector $D(\ell)$ at angular wavenumber ℓ, with mean of zero, and where we have used the non-mixing of angular wavenumber modes in equation (6) to simplify the expression. Subscripts α and β run over the set of parameters we are considering. $\Delta\Omega$ denotes the sky coverage area of the survey. We consider two types of data vector:

(i) For the shear only case, the data vector takes the form $D(\ell) = (\kappa_s^{(1)}(\ell), \ldots, \kappa_s^{(N_z)}(\ell))$, so that $C^{ij}(\ell) = P_{\kappa_s\kappa_s}^{(ij)}(\ell)$

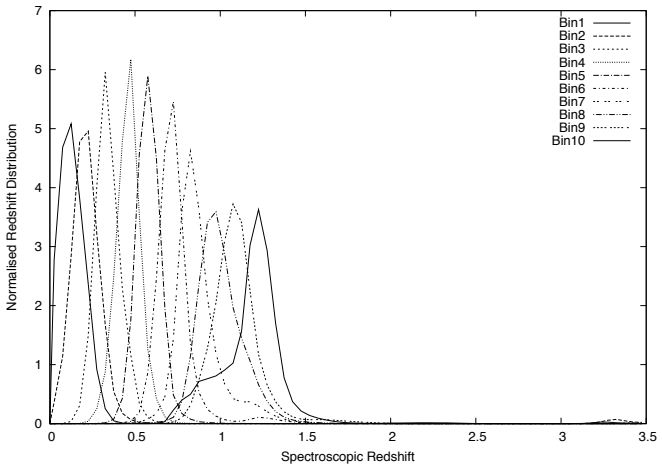

Figure 2. Galaxy Redshift distributions from CFHT data, including catastrophic redshifts for given galaxy sample selection and for all redshift bins. Should not be too busy by nature, as plots should only overlap in a small region.

(ii) For the combination of a shear analysis with information from magnification, the data vector takes the form $D(\ell) = (\kappa_s^{(1)}(\ell), \ldots, \kappa^{(N_z)}, \delta n^{(1)}(\ell), \ldots, \delta n^{(N_z)}(\ell))$ so that the covariance matrix takes block form

$$C(\ell) = \left(\begin{array}{c|c} P_{\kappa_s\kappa_s}(\ell) & P_{\kappa_s\delta n}(\ell) \\ \hline P_{\delta n\kappa_s}(\ell) & P_{\delta n\delta n}(\ell) \end{array}\right) \quad (25)$$

with Power Spectra as defined in equation (7).

Throughout this paper we utilise a Figure of Merit (FoM) as a measure of the constraining power of either analysis considered above, defined as

$$\mathrm{FoM_p} = \sqrt{\frac{1}{\det[F^{-1}]_p}} \quad (26)$$

where p denotes the subset of parameter space we are interested in.

3 MODELLING

3.1 Survey Modelling

3.2 Galaxy Bias

Including Priors on Galaxy Bias ref Appendix

4 DATA

Description of data

Derived Quantities

4.1 Optimisation

5 RESULTS

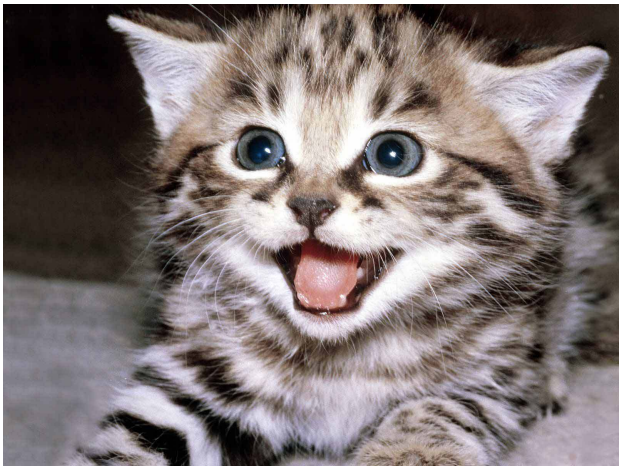

Figure 3. Shows alpha-1 as a function of magnitude for a given redshift bin/s

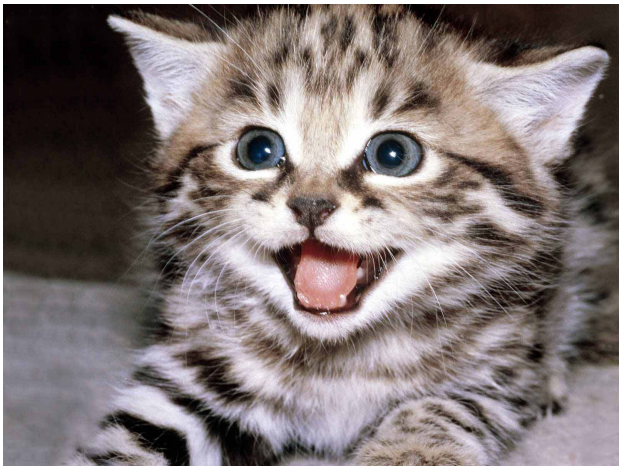

Figure 4. Cumulative number counts as a function of magnitude for a set of redshift bins, useful for discussion on level of effect when ignoring bright limit.

6 CONCLUSIONS

ACKNOWLEDGMENTS

REFERENCES

Bibliography here

APPENDIX A: ADDING A PRIOR ON GALAXY BIAS

This paper has been typeset from a TEX/ LATEX file prepared by the author.

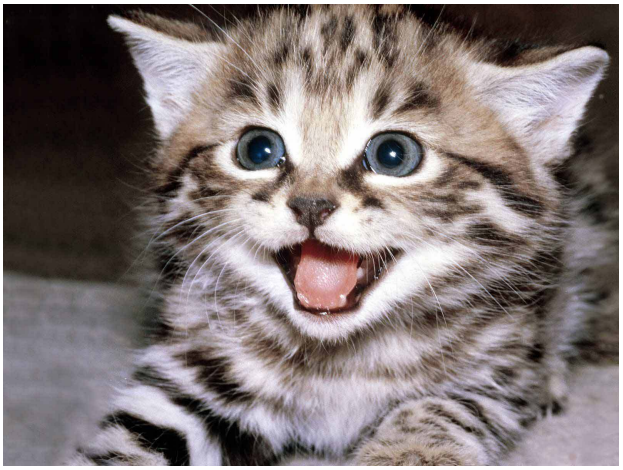

Figure 5. Signal to Noise plots for a selection of redshift bins (with errors) It is important to show these as a function of limiting magnitude to reinforce conclusion that optimisation requires deeper except in the case where limiting magnitude is in region where alpha-1 = 0.

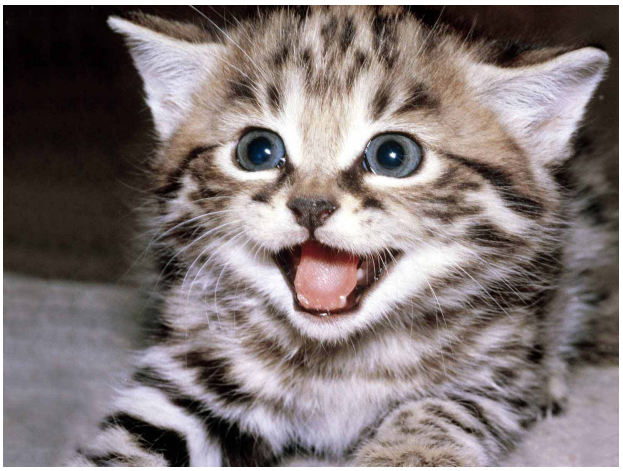

Figure 6. Alpha as a function of redshift for the redshift bins chosen, for magnitude limits motivated by previous signal to noise plot.

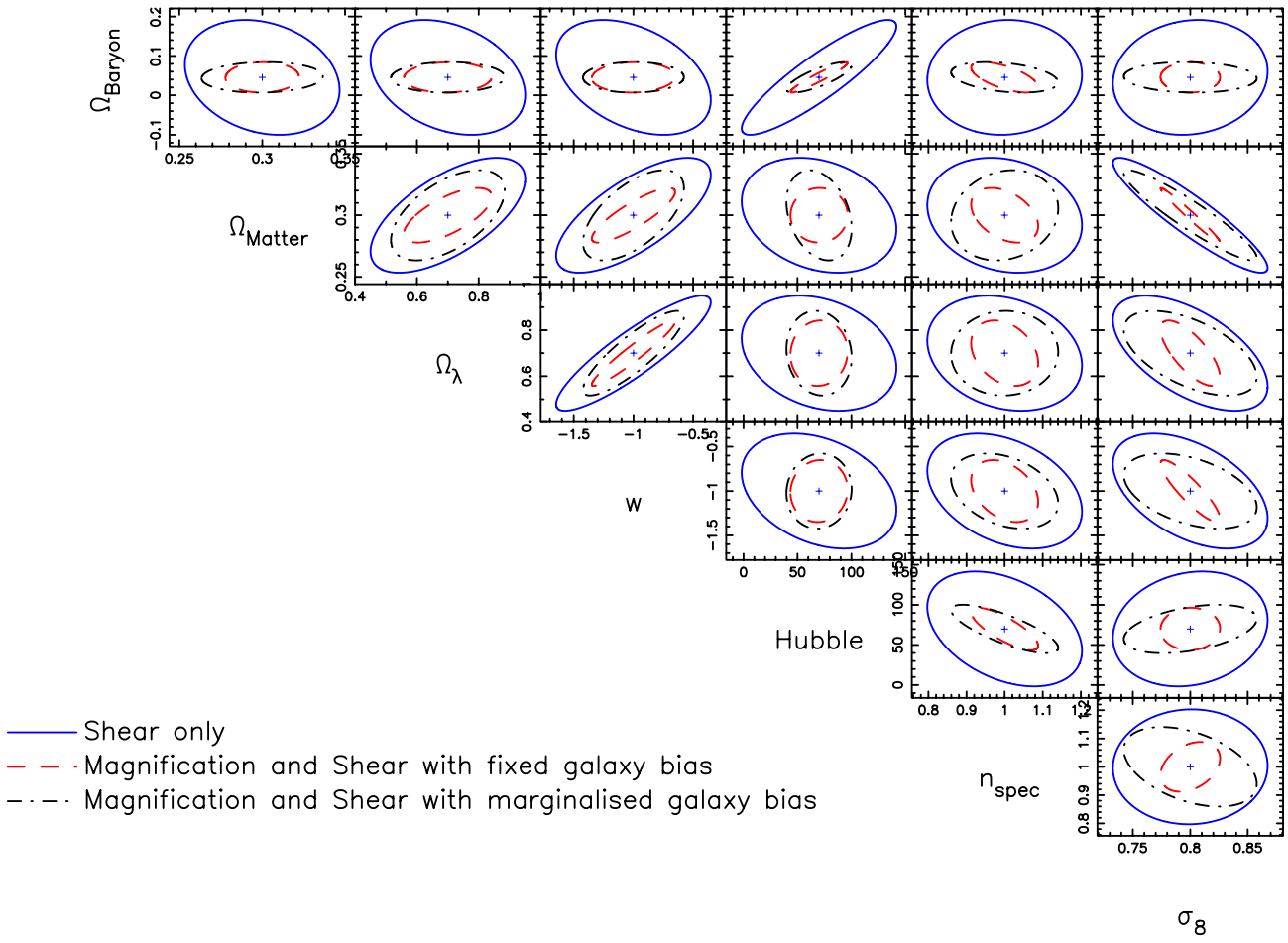

Figure 9. Contour plot showing fully optimised combined probe versus shear-only for choice of bias prior parameters.

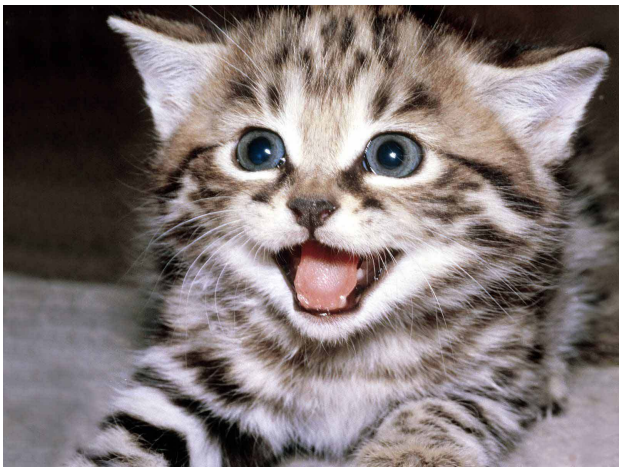

Figure 7. Contour plot for fully optimised magnifcation signal showing shear, and combined probe taking a known and fully unknown galaxy bias.

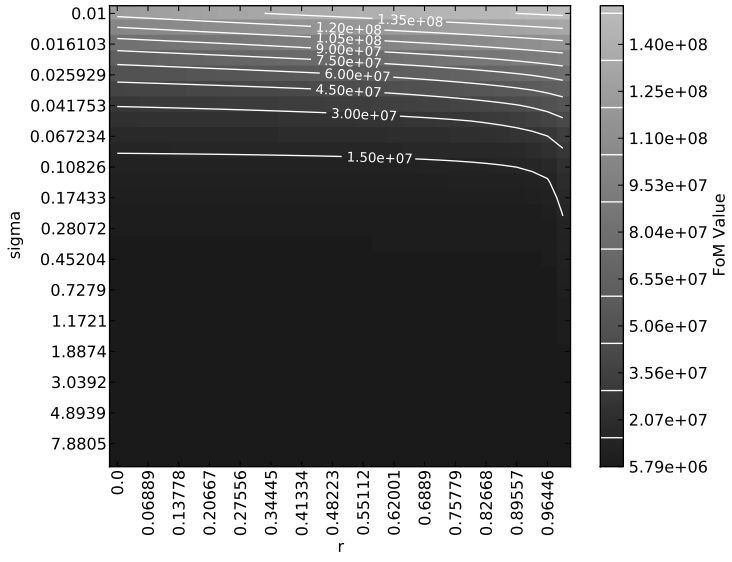

Figure 8. Contour plot showing constant-FoM contours as a function of σ and r (Uncertainty and correlation in Bias Prior). Point details choice of σ and r from external probe.

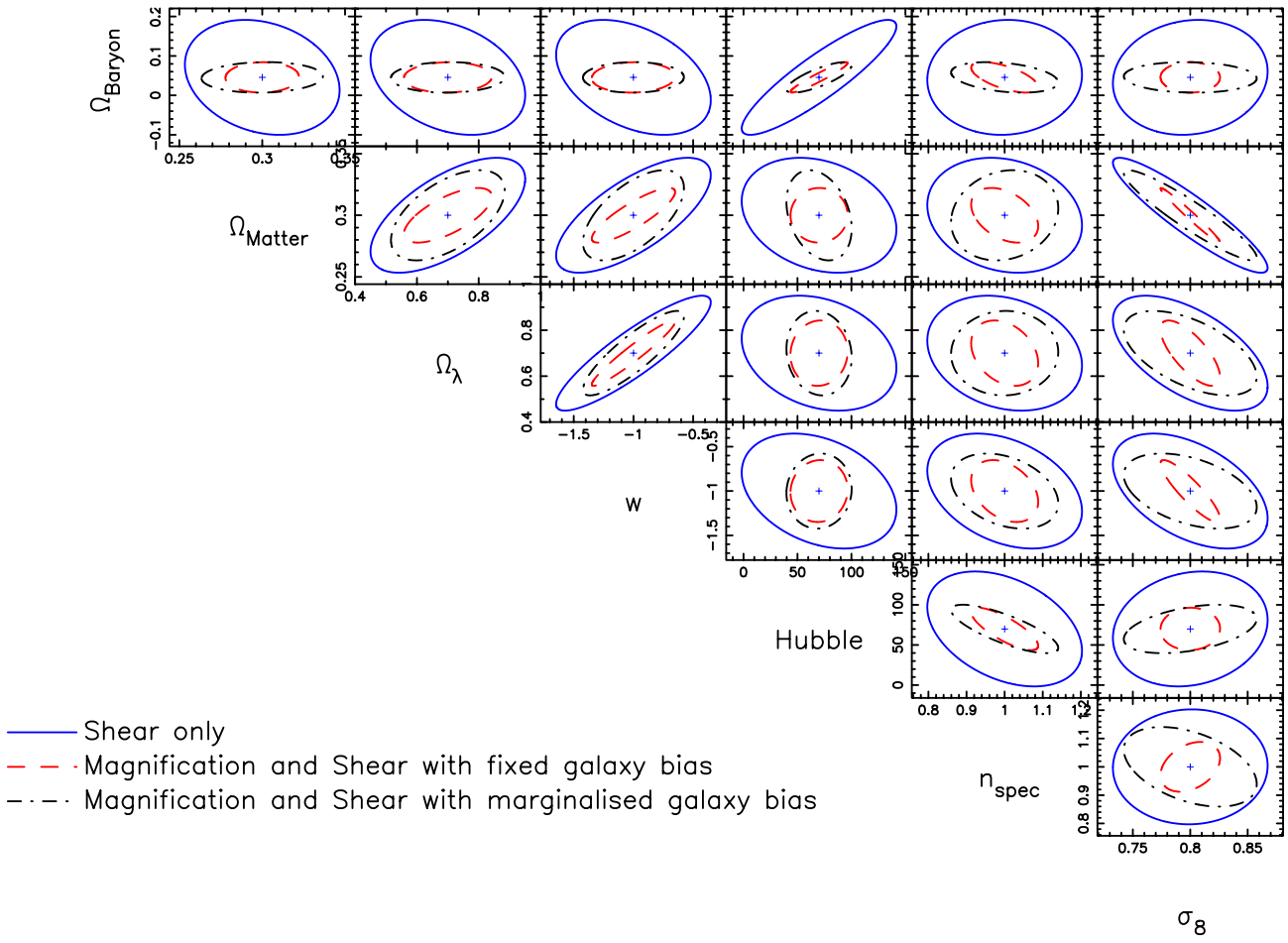

Figure 10. Contour plot showing fully optimised combined probe versus shear-only for choice of bias prior parameters with Planck Prior. - using old contour plot as placeholder

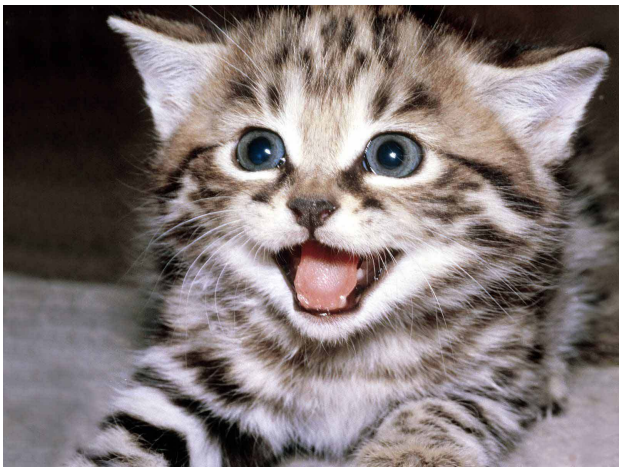

Figure 11. FoM vs number of redshift bins - gain in information by increasing redshift information - Optimisation.